3D Positioning with Unsynchronized LEO Satellites and Minimal Infrastructure

Don-Roberts Emenonye, Harpreet S. Dhillon, and R. Michael Buehrer

***Abstract*—In this paper, we rigorously derive the information in the signals received from low earth orbit (LEO) satellites, which are unsynchronized in time and frequency, and their utility for 3D position estimation. To enable this derivation, we define a system model that captures i) the time offset between LEOs caused by having cheap clocks, ii) the frequency offset between LEOs, and iii) multiple transmission time slots from a particular LEO. After this definition, we derive the Fisher information matrix (FIM) for the relevant channel parameters and transform the FIM for the channel parameters to the FIM for the 3D position. These derivations show the interactions between the number of LEOs, the operating frequency, the number of transmission time slots, and the number of receive antennas. Subsequently, these allow us to determine the minimal number of LEOs, the number of transmission time slots, and the number of receive antennas needed to determine the 3D position. One key result is that when the LEOs are unsynchronized in time and frequency and experience a high Doppler rate, the 3D position can be determined by observing a single LEO for four transmission time slots.**

I. Introduction

The race to provide low earth orbit (LEO) position, navigation, and timing services is on [1]. LEOs for localization can provide an alternative to the global navigation satellite system (GNSS) in the inevitable scenario when GNSS is unavailable or under attack from malicious sources. Research on LEO-based positioning ranges from dedicated [2]–[6] to semi-opportunistic to opportunistic techniques [7]–[16]. The authors in [2] propose a dedicated framework for utilizing broadband LEO constellations for navigation. The proposed framework utilizes delay measurements and is evaluated by considering the position errors as a function of the product of the geometric dilution of precision (GDOP) and the ranging errors. The ranging errors incorporate clock offset, and the orbit is assumed to be known, with the justification that the orbit can be accurately predicted by fifteen observing ground stations (just like the framework used in Galileo). This paper does not provide a theoretical FIM, experimental verification, and orientation and velocity estimation. In [3], a vision of a fused GNSS and dedicated LEO architecture in which existing clocks, modems, antennas, and spectrum of broadband satellite mega-constellations are dual-purposed for delay-based positioning.

D.-R. Emenonye, H. S. Dhillon, and R. M. Buehrer are with Wireless@VT, Bradley Department of Electrical and Computer Engineering, Virginia Tech, Blacksburg, VA, 24061, USA. Email: {donroberts, hdhillon, rbuehrer}@vt.edu. The support of the US National Science Foundation (Grants ECCS-2030215, CNS-1923807, and CNS-2107276) is gratefully acknowledged.

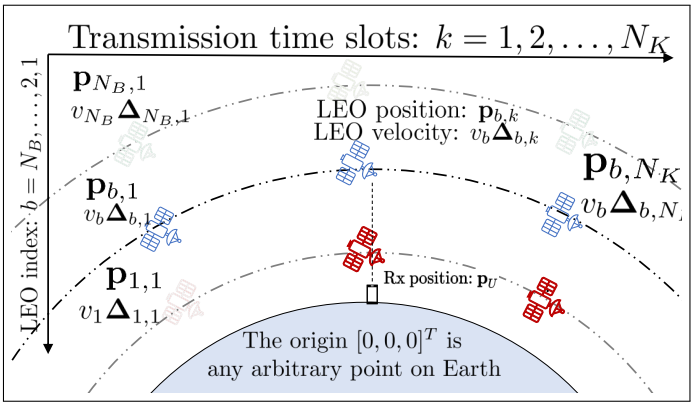

Figure 1. LEO-based localization systems with N_B LEOs transmitting during N_K transmission time slots to a receiver with N_U antennas.

In [4], the authors provide a dedicated framework for utilizing Doppler measurements from Amazon Kuiper Satellites are used for receiver positioning. Reference signal design for a dedicated framework using delay measurements is proposed in [5]. A dedicated framework is provided for massive MIMO-based integrated localization and communication, in which the delay and Doppler are used to position a receiver to improve the transmission rate in [6]. Authors in [7] design an experimental opportunistic framework to use eight Doppler measurements to find the position, velocity, and time offset of a receiver. In [8], measurements from Orbocmm satellites to track a receiver for 2 minutes. The authors in [9] develop a machine learning framework to estimate orbital parameters of an Orbocomm satellites. In [10], the reference signal from six Starlink satellites is acquired and used to position a receiver. In [12], a receiver is developed that combines signals from LEOs and 5G base stations to provide a position estimate. In [13], an Orbocomm satellite with a known orbit is observed at different time slots and used to position a receiver. In [14], the received signal frequency spectrum is mathematically characterized, a characterization that accounts for the high dynamic nature of the channel, which results from the speed of LEO satellites. A Doppler discriminator is proposed to differentiate between satellites, and a Doppler tracking algorithm is proposed. Finally, this opportunistic framework uses Doppler measurements to obtain a 2D position error of 4.3 m. The authors in [15] assume that the satellite's position and velocity are known, then a receiver is proposed. Subsequently, Doppler measurements from two Orbcomm satellites are used to position a receiver to an accuracy of 11 m opportunistically.

In [16], the spectrum of six LEO satellites is investigated. It was noticed that three of the satellites used tones while the other three used OFDM. The satellites were used to achieve a horizontal positioning error of 6.5 m opportunistically.

Although there has been some research on LEO-based positioning, the available information for LEO-based 3D position estimation needs to be rigorously characterized. Hence, in this paper, we utilize the Fisher information matrix (FIM) to derive the information needed for 3D positioning in the signals from unsynchronized LEOs (time and frequency) received during multiple transmission slots across multiple receive antennas. Moreover, the minimal infrastructure required to provide 3D position estimation is presented after simulations.

II. System Model

We consider N_B single antenna LEO satellites, each communicating with a receiver with N_U antennas, through transmissions in N_K different time slots. The transmission slots are spaced by Δ_t. At the k^{th} transmission time slot, the N_B LEO satellites are located at $\boldsymbol{p}_{b,k}, \quad b \in \{1, 2, \cdots, N_B\}$ and $k \in \{1, 2, \cdots, N_K\}$. The points, $\boldsymbol{p}_{b,k}$, are described with respect to a global origin. During the k^{th} time slot, the receiver has an arbitrary but known geometry with its centroid located at $\boldsymbol{p}_{U,k}$. During the k^{th} time slot, the point, $\boldsymbol{s}_u$, describes the u^{th} receive antenna with respect to the centroid while the point, $\boldsymbol{p}_{u,k}$, describes the position of this element with respect to the global origin as $\boldsymbol{p}_{u,k} = \boldsymbol{p}_{U,k} + \boldsymbol{s}_u$. The point, $\boldsymbol{s}_u$, can be written as $\boldsymbol{s}_u = \boldsymbol{Q}_U \tilde{\boldsymbol{s}}_u$ where $\tilde{\boldsymbol{s}}_u$ aligns with the global reference axis and $\boldsymbol{Q}_U = \boldsymbol{Q}(\alpha_U, \psi_U, \varphi_U)$ defines a 3D rotation matrix [17]. The orientation angles of the receiver are vectorized as $\boldsymbol{\Phi}_U = [\alpha_U, \psi_U, \varphi_U]^{\mathrm{T}}$. The centroid of the receiver at point, $\boldsymbol{p}_{U,k}$ with respect to the b^{th} LEO can be written as $\boldsymbol{p}_{U,k} = \boldsymbol{p}_{b,k} + d_{bU,k}\boldsymbol{\Delta}_{bU,k}$ where $d_{bU,k}$ is the distance from point $\boldsymbol{p}_{b,k}$ to point $\boldsymbol{p}_{U,k}$ and $\boldsymbol{\Delta}_{bU,k}$ is the corresponding unit direction vector $\boldsymbol{\Delta}_{bU,k} = [\cos\phi_{bU,k}\sin\theta_{bU,k}, \sin\phi_{bU,k}\sin\theta_{bU,k}, \cos\theta_{bU,k}]^{\mathrm{T}}$. During the k^{th} transmission time slot, the angles $\phi_{bU,k}$ and $\theta_{bU,k}$ represent the angle in the azimuth and elevation from the b^{th} LEO satellite to the receiver.

A. Transmit and Receive Processing

The N_B LEO satellites transmit in N_K different time slots, each of equal durations. At time t, during the k^{th} time slot, the b^{th} LEO satellite uses quadrature modulation and transmits the following signal to the receiver $x_{b,k}[t] = s_{b,k}[t]\exp(j2\pi f_c t)$, where $s_{b,k}[t]$ is the complex signal envelope of the signal transmitted by the b^{th} LEO satellite during the k^{th} time slot, and $f_c = c/\lambda$ is the operating frequency of LEO satellites. The speed of light is c, and λ is the operating wavelength. The channel model from the LEO satellites to the receiver consists only of the LOS paths. With this channel model and the transmit signal, the signal at the u^{th} receive antenna during the k^{th} time slot is

$$\begin{aligned} y_{u,k}[t] &= \sum_{b}^{N_B} y_{bu,k}[t], \\ &= \sum_{b=1}^{N_b} \beta_{bu,k}\sqrt{2}\Re\left\{s_{b,k}[t_{obu,k}]\exp(j(2\pi f_{ob,k}t_{obu,k}))\right\} \\ &\quad + n_{u,k}[t], \\ &= \mu_{u,k}[t] + n_{u,k}[t], \end{aligned} \tag{1}$$

where $\mu_{u,k}[t]$ and $n_{u,k}[t] \sim \mathcal{CN}(0, N_0)$ are the noise-free part (useful part) of the signal and the Fourier transformed thermal noise local to the receiver's antenna array, respectively. Also, $\beta_{bu,k}$ is the channel gain from the b^{th} LEO satellite observed at the u^{th} receive antenna during the k^{th} time slot, $f_{ob,k} = f_c(1-\nu_{b,k}) + \epsilon_b$ is the observed frequency at receiver with respect to the b^{th} LEO satellite, and $t_{obu,k} = t - \tau_{bu,k} + \delta_b$ is the effective time duration. In the observed frequency, $\nu_{b,k}$ is the Doppler with respect to the b^{th} LEO satellite, and ϵ_b is the frequency offset measured with respect to the b^{th} LEO satellite.

In the effective time duration, δ_b is the time offset at the receiver measured with respect to the b^{th} LEO satellite, and the delay from the u^{th} receive antenna to the b^{th} LEO satellite during the k^{th} time slot is $\tau_{bu,k} \triangleq \frac{\|\mathbf{p}_{u,k} - \mathbf{p}_{b,k}\|}{c}$.

Remark 1. *The unknown Doppler rate due to the speed of the LEOs is captured by the fact that the Doppler measurements, $\nu_{b,k}$, change every transmission time slot. In the subsequent sections, we will show that these changing Doppler measurements provide more degrees of freedom for localization. Also, the offset, δ_b, captures the unknown time offset as well as the unknown ionospheric and tropospheric delay concerning the b^{th} LEO satellite.*

Here, the position of the b^{th} LEO satellite and the u^{th} receive antenna during the k^{th} time slot is $\mathbf{p}_{b,k} = \mathbf{p}_{b,o} + \tilde{\mathbf{p}}_{b,k}$, and $\mathbf{p}_{u,k} = \mathbf{p}_{u,o} + \tilde{\mathbf{p}}_{U,k}$, respectively. Here, $\mathbf{p}_{b,o}$ and $\mathbf{p}_{u,o}$ are the reference points of the b^{th} LEO satellite and the u^{th} receive antenna, respectively. The distance travelled by the b^{th} LEO satellite and the u^{th} receive antenna are $\tilde{\mathbf{p}}_{b,k}$ and $\tilde{\mathbf{p}}_{u,k}$, respectively. These traveled distances can be described as $\tilde{\mathbf{p}}_{b,k} = (k-1)\Delta_t v_b \boldsymbol{\Delta}_{b,k}$, and $\tilde{\mathbf{p}}_{U,k} = (k-1)\Delta_t v_U \boldsymbol{\Delta}_{U,k}$, respectively. Here, v_b and v_U are speeds of the b^{th} LEO satellite and receiver, respectively. The associated directions are defined as $\boldsymbol{\Delta}_{b,k} = [\cos\phi_{b,k}\sin\theta_{b,k}, \sin\phi_{b,k}\sin\theta_{b,k}, \cos\theta_{b,k}]^{\mathrm{T}}$ and $\boldsymbol{\Delta}_{U,k} = [\cos\phi_{U,k}\sin\theta_{U,k}, \sin\phi_{U,k}\sin\theta_{U,k}, \cos\theta_{U,k}]^{\mathrm{T}}$, respectively. Now, the velocity of the b^{th} LEO satellite and the velocity of the receiver are $\boldsymbol{v}_{b,k} = v_b\boldsymbol{\Delta}_{b,k}$ and $\boldsymbol{v}_{U,k} = v_U\boldsymbol{\Delta}_{U,k}$, respectively. Hence, the Doppler observed by the receiver from the b^{th} LEO satellite is $\nu_{b,k} = \boldsymbol{\Delta}_{bU,k}^{\mathrm{T}}(\boldsymbol{v}_{b,k} - \boldsymbol{v}_{U,k})$.

B. Properties of the Received Signal

In this section, we discuss the properties that are observable in the signal at the receiver across all receive antennas and during all the transmission slots. To accomplish this, we consider the Fourier transform of the baseband signal that is transmitted by the b^{th} LEO satellite at time t during the k^{th} time slot $S_{b,k}[f] \triangleq \frac{1}{\sqrt{2\pi}} \int_{-\infty}^{\infty} s_{b,k}[t] \exp(-j2\pi f t) \ dt$. This Fourier transform is called the spectral density.

1) Effective Baseband Bandwidth: This can be viewed as the average of the squared of all frequencies normalized by the area occupied by the spectral density, $S_{b,k}$. Mathematically, the effective baseband bandwidth is $\alpha_{1b,k} \triangleq \left(\frac{\int_{-\infty}^{\infty} f^2 |S_{b,k}[f]|^2 df}{\int_{-\infty}^{\infty} |S_{b,k}[f]|^2 df} \right)^{\frac{1}{2}}$.

2) Baseband-Carrier Correlation (BCC): Mathematically, the BCC is $\alpha_{2b,k} \triangleq \frac{\int_{-\infty}^{\infty} f |S_{b,k}[f]|^2 df}{\left(\int_{-\infty}^{\infty} f^2 |S_{b,k}[f]|^2 df\right)^{\frac{1}{2}} \left(\int_{-\infty}^{\infty} |S_{b,k}[f]|^2 df\right)^{\frac{1}{2}}}$. In later sections, the term $\alpha_{2b,k}$ will help provide a compact representation of the mathematical description of the available information in the received signals.

3) Received Signal-to-Noise Ratio: The SNR is the ratio of the power of the signal across its occupied frequencies to the noise spectral density. Mathematically, the SNR is $\underset{bu,k}{\text{SNR}} \triangleq \frac{8\pi^2 |\beta_{bu,k}|^2}{N_0} \int_{-\infty}^{\infty} |S_{b,k}[f]|^2 \, df$.

The mathematical description of the available information useful for 3D positioning is written in terms of these received signal properties.

III. Available Information in the Received Signal

In this section, we define the parameters, both geometric channel parameters and nuisance parameters. The definition of these parameters serves as an intermediate step to investigating the available geometric information provided by LEOs, which subsequently helps the investigation of the feasibility of LEO-based localization under different types of LEO constellations, number of LEOs, beam split, and number of receive antennas.

A. Error Bounds on Parameters

The analysis in this section is based on the received signal given by (1), which is obtained from N_B LEO satellites on N_U receive antennas during N_K distinct time slots of T durations each. The parameters observable in the signal received by a receiver from the b^{th} LEO satellite on its N_U receive antenna during the N_K different time slots are subsequently presented. The delays observed across the N_U receive antennas during the k^{th} time slots are presented in vector form $\boldsymbol{\tau}_{b,k} \triangleq [\tau_{b1,k}, \tau_{b2,k}, \cdots, \tau_{bN_U,k}]^{\mathrm{T}}$, then the delays across the N_U receive antennas during all N_K time slots are also vectorized as follows $\boldsymbol{\tau}_b \triangleq \left[\boldsymbol{\tau}_{b,1}^{\mathrm{T}}, \boldsymbol{\tau}_{b,2}^{\mathrm{T}}, \cdots, \boldsymbol{\tau}_{b,N_K}^{\mathrm{T}}\right]^{\mathrm{T}}$.The Doppler observed with respect to the b^{th} LEO satellite across all the N_K transmission time slots is $\boldsymbol{\nu}_b \triangleq [\nu_{b,1}, \nu_{b,2}, \cdots, \nu_{b,N_K}]^{\mathrm{T}}$. Next, the channel gain across the N_U receive antennas during the k^{th} time slots are presented in vector form $\boldsymbol{\beta}_{b,k} \triangleq [\beta_{b1,k}, \beta_{b2,k}, \cdots, \beta_{bN_U,k}]^{\mathrm{T}}$, then the delays across the N_U receive antennas during all N_K time slots are also vectorized as follows $\boldsymbol{\beta}_b \triangleq \left[\boldsymbol{\beta}_{b,1}^{\mathrm{T}}, \boldsymbol{\beta}_{b,2}^{\mathrm{T}}, \cdots, \boldsymbol{\beta}_{b,N_K}^{\mathrm{T}}\right]^{\mathrm{T}}$. Note that if there is no beam split, the channel gain remains constant across all antennas and is simply $\boldsymbol{\beta}_b \triangleq \left[\beta_{b,1}, \beta_{b,2}, \cdots, \beta_{b,N_K}\right]^{\mathrm{T}}$. Moreover, if the channel gain is constant across all time slots, we can further represent the b^{th} LEO transmission by the scalar, β_b. Finally, with these vectorized forms, the total parameters observable in the signals received at a receiver from the b^{th} LEO satellite on its N_U receive antenna during the N_K different time slots are vectorized as follows $\boldsymbol{\eta}_b^{\mathrm{T}} \triangleq \left[\boldsymbol{\tau}_b^{\mathrm{T}}, \boldsymbol{\nu}_b^{\mathrm{T}}, \boldsymbol{\beta}_b^{\mathrm{T}}, \delta_b, \epsilon_b\right]^{\mathrm{T}}$. All signals observable from all N_B LEO satellites across N_U receive antennas during the N_K different time slots are vectorized as $\boldsymbol{\eta}^{\mathrm{T}} \triangleq \left[\boldsymbol{\eta}_1^{\mathrm{T}}, \boldsymbol{\eta}_2^{\mathrm{T}}, \cdots, \boldsymbol{\eta}_{N_B}^{\mathrm{T}}\right]^{\mathrm{T}}$. After specifying the parameters that are present in the signals received from the LEO satellites - considering the time slots and receive antennas, we present the mathematical preliminaries needed for further discussions.

B. Mathematical Preliminaries

Although we have specified the parameters in the signals received in a LEO-based localization system, we still have to investigate the estimation accuracy achievable when estimating these parameters. Moreover, it's unclear whether all the parameters presented are separately observable and can contribute to a localization framework. One way of answering these two questions is by using the FIM.

Definition 1. *The general FIM for a parameter vector, $\boldsymbol{\eta}$, defined as $\mathbf{J}_{\boldsymbol{y};\boldsymbol{\eta}} = \boldsymbol{F}_{\boldsymbol{y};\boldsymbol{\eta}}(\boldsymbol{y};\boldsymbol{\eta};\boldsymbol{\eta},\boldsymbol{\eta})$ is the summation of the FIM obtained from the likelihood due to the observations defined as $\mathbf{J}_{\boldsymbol{y}|\boldsymbol{\eta}} = \boldsymbol{F}_{\boldsymbol{y}}(\boldsymbol{y}|\boldsymbol{\eta};\boldsymbol{\eta},\boldsymbol{\eta})$ and the FIM from* a priori *information about the parameter vector defined as $\mathbf{J}_{\boldsymbol{\eta}} = \boldsymbol{F}_{\boldsymbol{\eta}}(\boldsymbol{\eta};\boldsymbol{\eta},\boldsymbol{\eta})$. In mathematical terms, we have*

$$\begin{aligned} \mathbf{J}_{\boldsymbol{y};\boldsymbol{\eta}} &\triangleq -\mathbb{E}_{\boldsymbol{y};\boldsymbol{\eta}} \left[\frac{\partial^2 \ln \chi(\boldsymbol{y};\boldsymbol{\eta})}{\partial \boldsymbol{\eta} \partial \boldsymbol{\eta}^{\mathrm{T}}} \right] \\ &= -\mathbb{E}_{\boldsymbol{y}} \left[\frac{\partial^2 \ln \chi(\boldsymbol{y}|\boldsymbol{\eta})}{\partial \boldsymbol{\eta} \partial \boldsymbol{\eta}^{\mathrm{T}}} \right] - \mathbb{E}_{\boldsymbol{\eta}} \left[\frac{\partial^2 \ln \chi(\boldsymbol{\eta})}{\partial \boldsymbol{\eta} \partial \boldsymbol{\eta}^{\mathrm{T}}} \right] \\ &= \mathbf{J}_{\boldsymbol{y}|\boldsymbol{\eta}} + \mathbf{J}_{\boldsymbol{\eta}}, \end{aligned} \tag{2}$$

where $\chi(\boldsymbol{y};\boldsymbol{\eta})$ denotes the probability density function (PDF) of $\boldsymbol{y}$ and $\boldsymbol{\eta}$.

Definition 2. *Given a parameter vector, $\boldsymbol{\eta} \triangleq \left[\boldsymbol{\eta}_1^{\mathrm{T}}, \boldsymbol{\eta}_2^{\mathrm{T}}\right]^{\mathrm{T}}$, where $\boldsymbol{\eta}_1$ is the parameter of interest, the resultant FIM has the structure*

$$\mathbf{J}_{\boldsymbol{y};\boldsymbol{\eta}} = \begin{bmatrix} \mathbf{J}_{\boldsymbol{y};\boldsymbol{\eta}_1} & \mathbf{J}_{\boldsymbol{y};\boldsymbol{\eta}_1,\boldsymbol{\eta}_2} \\ \mathbf{J}_{\boldsymbol{y};\boldsymbol{\eta}_1,\boldsymbol{\eta}_2}^{\mathrm{T}} & \mathbf{J}_{\boldsymbol{y};\boldsymbol{\eta}_2} \end{bmatrix},$$

where $\boldsymbol{\eta} \in \mathbb{R}^N, \boldsymbol{\eta}_1 \in \mathbb{R}^n, \mathbf{J}_{\boldsymbol{y};\boldsymbol{\eta}_1} \in \mathbb{R}^{n \times n}, \mathbf{J}_{\boldsymbol{y};\boldsymbol{\eta}_1,\boldsymbol{\eta}_2} \in \mathbb{R}^{n \times (N-n)}$, and $\mathbf{J}_{\boldsymbol{y};\boldsymbol{\eta}_2} \in \mathbb{R}^{(N-n) \times (N-n)}$ with $n < N$, and the EFIM [18] of parameter $\boldsymbol{\eta}_1$ is given by $\mathbf{J}_{\boldsymbol{y};\boldsymbol{\eta}_1}^{\mathrm{e}} = \mathbf{J}_{\boldsymbol{y};\boldsymbol{\eta}_1} - \mathbf{J}_{\boldsymbol{y};\boldsymbol{\eta}_1}^{nu} = \mathbf{J}_{\boldsymbol{y};\boldsymbol{\eta}_1} - \mathbf{J}_{\boldsymbol{y};\boldsymbol{\eta}_1,\boldsymbol{\eta}_2} \mathbf{J}_{\boldsymbol{y};\boldsymbol{\eta}_2}^{-1} \mathbf{J}_{\boldsymbol{y};\boldsymbol{\eta}_1,\boldsymbol{\eta}_2}^{\mathrm{T}}$.

C. Fisher Information Matrix for Channel Parameters

In the definitions of the FIM and EFIM given in the previous section, the expression of the likelihood of the received signal conditioned on the parameter vector is required. This

likelihood for the received signal conditioned on the parameter vector is defined considering the N_B LEO satellites, N_U receive antennas, and the N_K time slots, and is presented next.

$$\chi(\boldsymbol{y}[t]|\boldsymbol{\eta}) \propto \prod_{b=1}^{N_B}\prod_{u=1}^{N_U}\prod_{k=1}^{N_K} \exp\left\{\frac{2}{N_0}\int_0^T \Re\left\{\mu_{bu,k}^{\mathrm{H}}[t]y_{bu,k}[t]\right\}dt - \frac{1}{N_0}\int_0^T |\mu_{bu,k}[t]|^2\,dt\right\}. \tag{3}$$

Subsequently, this FIM due to the observations from the N_B LEO satellite, received across the N_U antennas, and during the N_K distinct time slots can be computed with the likelihood function (3) and Definition 1, and it results in the diagonal matrix[1]. $\mathbf{J}_{\boldsymbol{y}|\boldsymbol{\eta}} = \boldsymbol{F}_{\boldsymbol{y}}(\boldsymbol{y}|\boldsymbol{\eta};\boldsymbol{\eta},\boldsymbol{\eta}) = \mathrm{diag}\left\{\boldsymbol{F}_{\boldsymbol{y}}(\boldsymbol{y}|\boldsymbol{\eta};\boldsymbol{\eta}_1,\boldsymbol{\eta}_1),\ldots,\boldsymbol{F}_{\boldsymbol{y}}(\boldsymbol{y}|\boldsymbol{\eta};\boldsymbol{\eta}_{N_B},\boldsymbol{\eta}_{N_B})\right\}$. The entries in FIM due to the observations of the received signals from b^{th} LEO satellite can be obtained through the simplified expression. $\boldsymbol{F}_{\boldsymbol{y}}(\boldsymbol{y}|\boldsymbol{\eta};\boldsymbol{\eta}_b,\boldsymbol{\eta}_b) = \frac{1}{N_0}\sum_{u,k}^{N_U N_K}\Re\left\{\int \nabla_{\boldsymbol{\eta}_b}\mu_{bu,k}[t]\nabla_{\boldsymbol{\eta}_b}\mu_{bu,k}^{\mathrm{H}}[t]\;dt\right\}$. The non-zero elements in the FIM are presented next. Considering the b^{th} LEO satellite, the FIM focusing on the delays at the u^{th} receive antenna during the k^{th} time slot is $\boldsymbol{F}_{\boldsymbol{y}}(\boldsymbol{y}|\boldsymbol{\eta};\tau_{bu,k},\tau_{bu,k}) = -\boldsymbol{F}_{\boldsymbol{y}}(\boldsymbol{y}|\boldsymbol{\eta};\tau_{bu,k},\delta_b) = \underset{bu,k}{\mathrm{SNR}}\omega_{b,k}$. where $\omega_{b,k} = \begin{bmatrix}\alpha_{1b,k}^2 + 2f_{ob,k}\alpha_{1b,k}\alpha_{2b,k} + f_{ob,k}^2\end{bmatrix}$.

The FIM focusing on the Doppler observed with respect to the b^{th} LEO satellite at the receiver during the k^{th} time slot is presented next. The FIM of the Doppler observed with respect to the b^{th} LEO satellite at the receiver during the k^{th} time slot is $\boldsymbol{F}_{\boldsymbol{y}}(\boldsymbol{y}|\boldsymbol{\eta};\nu_{b,k},\nu_{b,k}) = 0.5 * \underset{bu,k}{\mathrm{SNR}} f_c^2 t_{obu,k}^2$. The FIM of the Doppler observed with respect to the b^{th} LEO satellite and the corresponding frequency offset during the k^{th} time slot is $\boldsymbol{F}_{\boldsymbol{y}}(\boldsymbol{y}|\boldsymbol{\eta};\nu_{b,k},\epsilon_b) = -0.5 * \underset{bu,k}{\mathrm{SNR}} f_c t_{obu,k}^2$.

The FIM of the channel gain in the FIM due to the observations of the received signals from b^{th} LEO satellite to the u^{th} receive antenna during the k^{th} time slot is $\boldsymbol{F}_{\boldsymbol{y}}(\boldsymbol{y}|\boldsymbol{\eta};\beta_{bu,k},\beta_{bu,k}) = \frac{1}{4\pi^2|\beta_{bu,k}|^2}\underset{bu,k}{\mathrm{SNR}}$.

The FIM focusing on the time offset at the u^{th} receive antenna during the k^{th} time slot with respect to the b^{th} LEO satellite is presented next. The FIM of the time offset in the FIM due to the observations of the received signals from b^{th} LEO satellite to the u^{th} receive antenna during the k^{th} time slot is

$$\boldsymbol{F}_{\boldsymbol{y}}(\boldsymbol{y}|\boldsymbol{\eta};\delta_b,\delta_b) = \boldsymbol{F}_{\boldsymbol{y}}(\boldsymbol{y}|\boldsymbol{\eta};\tau_{bu,k},\tau_{bu,k}) = -\boldsymbol{F}_{\boldsymbol{y}}(\boldsymbol{y}|\boldsymbol{\eta};\delta_b,\tau_{bu,k}).$$

The FIM focusing on the frequency offset at the u^{th} receive antenna during the k^{th} time slot with respect to the b^{th} LEO satellite is presented next. The FIM of the frequency offset in the FIM due to the observations of the received signals from b^{th} LEO satellite to the u^{th} receive antenna during the k^{th} time slot is

$$\boldsymbol{F}_{\boldsymbol{y}}(\boldsymbol{y}|\boldsymbol{\eta};\epsilon_b,\epsilon_b) = 0.5 * \underset{bu,k}{\mathrm{SNR}} t_{obu,k}^2.$$

The FIM of the channel parameters, based on the observations of the received signals, is used to derive the FIM of the receiver's 3D position in the next section.

IV. Fisher Information Matrix for Location Parameters

In the previous section, we highlighted the useful and nuisance parameters present in the signals received from the N_B LEO satellites across the N_U receive antennas during N_K different time slots. Subsequently, we derived the information about these parameters present in the received signals and presented the structure of these parameters. In this section, we use the FIM for channel parameters to derive the FIM for the location parameters and highlight the FIM structure. This FIM for the location parameters will determine how feasible it is to find the 3D position of a receiver with the signals received from LEO satellites.

To proceed, we define $\boldsymbol{p}_U = \boldsymbol{p}_{U,0}$ and the location parameters $\boldsymbol{\kappa} = [\boldsymbol{p}_U, \boldsymbol{\zeta}_1, \boldsymbol{\zeta}_2, \cdots, \boldsymbol{\zeta}_{N_B}]$, where $\boldsymbol{\zeta}_b = \left[\boldsymbol{\beta}_b^{\mathrm{T}}, \delta_b, \epsilon_b\right]^{\mathrm{T}}$, and our goal is to derive the FIM of the entire location parameter vector, or different combinations of parameters, under different levels of uncertainty about the channel parameters. The FIM for the location parameters, $\mathbf{J}_{\boldsymbol{y}|\boldsymbol{\kappa}}$ can be obtained from the FIM for the channel parameters, $\mathbf{J}_{\boldsymbol{y}|\boldsymbol{\eta}}$, using the bijective transformation $\mathbf{J}_{\boldsymbol{y}|\boldsymbol{\kappa}} \triangleq \boldsymbol{\Upsilon}_{\boldsymbol{\kappa}}\mathbf{J}_{\boldsymbol{y}|\boldsymbol{\eta}}\boldsymbol{\Upsilon}_{\boldsymbol{\kappa}}^{\mathrm{T}}$, where $\boldsymbol{\Upsilon}_{\boldsymbol{\kappa}}$ represents derivatives of the non-linear relationship between the geometric channel parameters, $\boldsymbol{\eta}$, and the location parameters [19]. The elements in the bijective transformation matrix $\boldsymbol{\Upsilon}_{\boldsymbol{\kappa}}$ are given in Appendix A. With no *a priori* information about the location parameters $\boldsymbol{\kappa}$, $\mathbf{J}_{\boldsymbol{y};\boldsymbol{\kappa}} = \mathbf{J}_{\boldsymbol{y}|\boldsymbol{\kappa}}$. The EFIM taking $\boldsymbol{\kappa}_1 = \boldsymbol{p}_U$ as the parameter of interest and $\boldsymbol{\kappa}_2 = [\boldsymbol{\zeta}_1, \boldsymbol{\zeta}_2, \cdots, \boldsymbol{\zeta}_{N_B}]$ as the nuisance parameters is now derived.

A. Elements in $\mathbf{J}_{\boldsymbol{y};\boldsymbol{\kappa}_1}$

The elements in $\mathbf{J}_{\boldsymbol{y};\boldsymbol{\kappa}_1}$ are presented through the following Lemmas. This FIM corresponds to the available information of the location parameters $\boldsymbol{\kappa}_1$ when the nuisance parameters are known.

Lemma 1. *The FIM of the 3D position of the receiver is*

$$\boldsymbol{F}_y(\boldsymbol{y}|\boldsymbol{\eta};\boldsymbol{p}_U,\boldsymbol{p}_U) = \sum_{b,k,u}\underset{bu,k}{\mathrm{SNR}}\left[\frac{\omega_{b,k}}{c^2}\boldsymbol{\Delta}_{bu,k}\boldsymbol{\Delta}_{bu,k}^{\mathrm{T}} + \frac{f_c^2 t_{obu,k}^2 \nabla_{\boldsymbol{p}_U}\nu_{b,k}\nabla_{\boldsymbol{p}_U}^{\mathrm{T}}\nu_{b,k}}{2}\right]. \tag{4}$$

B. Elements in $\mathbf{J}_{\boldsymbol{y};\boldsymbol{\kappa}_1}^{nu}$

The elements in $\mathbf{J}_{\boldsymbol{y};\boldsymbol{\kappa}_1}^{nu}$ are presented in this section. These elements represent the loss of information about $\boldsymbol{\kappa}_1$ due to uncertainty in the nuisance parameters $\boldsymbol{\kappa}_2$.

[1]With the assumption that the parameters from different LEO satellites are independent.

$$\begin{aligned}\mathbf{J}^{\mathrm{e}}_{\boldsymbol{y};\boldsymbol{p}_U} &= [\mathbf{J}^{\mathrm{e}}_{\boldsymbol{y};\boldsymbol{\kappa}_1}]_{[1:3,1:3]} = \boldsymbol{F}_y(\boldsymbol{y}|\boldsymbol{\eta};\boldsymbol{p}_U,\boldsymbol{p}_U) - \boldsymbol{G}_y(\boldsymbol{y}|\boldsymbol{\eta};\boldsymbol{p}_U,\boldsymbol{p}_U) \\ &= \sum_{b,k,u} \underset{bu,k}{\mathrm{SNR}} \left[\frac{\omega_{b,k}}{c^2} \boldsymbol{\Delta}_{bu,k} \boldsymbol{\Delta}^{\mathrm{T}}_{bu,k} + \frac{f_c^2 t^2_{obu,k} \nabla_{\boldsymbol{p}_U} \nu_{b,k} \nabla^{\mathrm{T}}_{\boldsymbol{p}_U} \nu_{b,k}}{2} \right] \\ &- \left[\sum_b \frac{1}{c^2} \left\| \sum_{k,u} \underset{bu,k}{\mathrm{SNR}} \boldsymbol{\Delta}^{\mathrm{T}}_{bu,k} \omega_{b,k} \right\|^2 \left(\sum_{u,k} \underset{bu,k}{\mathrm{SNR}} \omega_{b,k} \right)^{-1} + \sum_b \left\| \sum_{k,u} \underset{bu,k}{\mathrm{SNR}} \ \nabla^{\mathrm{T}}_{\boldsymbol{p}_U} \nu_{b,k} \frac{(f_c)(t^2_{obu,k})}{2} \right\|^2 \left(\sum_{u,k} \frac{\underset{bu,k}{\mathrm{SNR}} t^2_{obu,k}}{2} \right)^{-1} \right].\end{aligned} \tag{6}$$

Lemma 2. *The loss of information about 3D position of the receiver due to uncertainty in the nuisance parameters $\boldsymbol{\kappa}_2$ is*

$$\begin{aligned}\boldsymbol{G}_y(\boldsymbol{y}|\boldsymbol{\eta};\boldsymbol{p}_U,\boldsymbol{p}_U) =& \sum_b \left\| \sum_{k,u} \underset{bu,k}{\mathrm{SNR}} \boldsymbol{\Delta}^{\mathrm{T}}_{bu,k} \frac{\omega_{b,k}}{c} \right\|^2 \left(\sum_{u,k} \underset{bu,k}{\mathrm{SNR}} \omega_{b,k} \right)^{-1} \\ &+ \sum_b \left\| \sum_{k,u} \underset{bu,k}{\mathrm{SNR}} \ \nabla^{\mathrm{T}}_{\boldsymbol{p}_U} \nu_{b,k} \frac{(f_c)(t^2_{obu,k})}{2} \right\|^2 \left(\sum_{u,k} \frac{\underset{bu,k}{\mathrm{SNR}} t^2_{obu,k}}{2} \right)^{-1}\end{aligned} \tag{5}$$

The elements in the EFIM for the location parameters, $\mathbf{J}^{\mathrm{e}}_{\boldsymbol{y};\boldsymbol{\kappa}_1}$ are obtained by appropriately combining the Lemmas in Section IV-A and the Lemmas in Section IV-B. The EFIM for the location parameters is

$$\mathbf{J}^{\mathrm{e}}_{\boldsymbol{y};\boldsymbol{\kappa}_1} = \mathbf{J}_{\boldsymbol{y};\boldsymbol{\kappa}_1} - \mathbf{J}^{nu}_{\boldsymbol{y};\boldsymbol{\kappa}_1} = \mathbf{J}_{\boldsymbol{y};\boldsymbol{\kappa}_1} - \mathbf{J}_{\boldsymbol{y};\boldsymbol{\kappa}_1,\boldsymbol{\kappa}_2} \mathbf{J}^{-1}_{\boldsymbol{y};\boldsymbol{\kappa}_2} \mathbf{J}^{\mathrm{T}}_{\boldsymbol{y};\boldsymbol{\kappa}_1,\boldsymbol{\kappa}_2}.$$

Here, we consider available information for estimating the 3D position. This information is specified by the EFIM of the 3D position of the receiver and is given by (6).

V. Numerical Results

This section presents simulation results that describe the available information in signals received from LEO satellites during multiple transmission time slots on receivers with multiple antennas. We start by showing the minimum infrastructure needed to estimate the 3D position. More specifically, we present the minimum number of LEO satellites, time slots, and receive antennas that contribute to 3D position estimation. We also present the Cramer Rao bound (CRB) for 3D position as a function of the spacing between transmission time slots.

We use the following simulation parameters. The SNR is assumed constant across the transmission time slots and receive antennas, and the following set of SNR values is considered: $\{40 \text{ dB}, 20 \text{ dB}, 0 \text{ dB}, -20 \text{ dB}\}$. The x,y, and z components of the position of the LEO satellites are randomly chosen, but LEO satellites are approximately 2000 km from the receiver. The x,y, and z components of the velocity of the LEO satellites are randomly chosen and change every transmission time slot to depict acceleration, but the LEO satellites have a speed of 8000 m/s. The receiver's position's x,y, and z components are randomly chosen, but the receiver is approximately 30 m from the origin. The x,y, and z components of the receiver's velocity are randomly chosen and remain constant to depict constant velocity, but the receiver has a speed of 25 m/s. The effective baseband bandwidth, $\alpha_{1b,k}$, is 100 MHz and the BCC, $\alpha_{2b,k}$, is 0 MHz.

A. 3D Position Estimation

Here, we investigate the minimal number of time slots, LEO satellites, and receive antennas that produce a positive definite FIM for the 3D position of the receiver, which is defined by (6). We start with the cases where we only have measurements taken during a single time slot from various LEO satellites considering single or multiple antennas.

1) $N_K = 1$, $N_B = 1$, and $N_U > 1$: Under this condition, the information is insufficient to find the 3D position of the receiver when there is a time offset. However, without a time offset, the information is enough to find the 3D position of the receiver. The 3D position of the receiver can be obtained by combining the available TOA measurements from the single LEO satellite with the multiple receive antennas.

2) $N_K = 1$, $N_B = 2$, and $N_U = 1$: Under this condition, the information is insufficient to find the 3D position of the receiver when there is a time offset, a frequency offset, or both. However, without a time offset or frequency offset, the information is enough to find the 3D position of the receiver. These can be done with two TOAs from two LEO satellites and a single Doppler measurement from either of the two LEO satellites or with two Dopplers from two LEO satellites and a single TOA measurement from either of the two LEO satellites.

3) $N_K = 1$, $N_B = 2$, and $N_U > 1$: Under this condition, the information is insufficient to find the 3D position of the receiver when there is a time offset, a frequency offset, or both. Without a time offset or frequency offset, the 3D position can be found using: i) two TOA measurements from two distinct LEOs and a Doppler measurement from either of the LEO, ii) two Doppler measurements from two distinct LEOs and a TOA measurement from either of the LEO satellites, iii) two unit vectors from two distinct LEOs obtainable due to the presence of multiple receive antennas, which capture multiple TOAs from a single LEO satellite, iv) one TOA measurement from a distinct LEO and a unit vector from the other LEO satellites, and v) one Doppler measurement from a distinct LEO and a unit vector from the other LEO.

4) $N_K = 1$, $N_B = 3$, and $N_U = 1$: Under this condition, the information is insufficient to find the 3D position of the receiver when both a time offset and frequency offset are present. Without a time offset and frequency offset, the 3D position can be found using: i) three TOA measurements from three distinct LEO satellites, ii) three Doppler measurements from three distinct LEO satellites, iii) two TOA measurements from two distinct LEOs and Doppler measurement from either of the LEO, and iv) two Doppler measurements from two

distinct LEOs and a TOA measurement from either of the LEO satellites. With only a time offset, ii) can be used to find the 3D position, while with only a frequency offset, i) can be utilized to find the 3D position.

Now, we focus on the cases when we only have measurements taken from a single LEO satellite considering single and multiple receive antennas, and different number of time slots.

5) $N_K = 2$, $N_B = 1$, and $N_U = 1$: Under this condition, the presence of either a time or frequency offset means there is insufficient information to find the 3D position of the receiver. Without a time and frequency offset, there is enough information to find the 3D position of the receiver using: i) two TOAs from the same LEO satellite obtained during two distinct time slots in combination with the Doppler measurements obtained during either of the time slots with respect to the LEO satellite, and ii) two Doppler measurements obtained during the two distinct time slots with respect to the LEO satellite in combination with the TOA obtained during either of the time slots.

6) $N_K = 2$, $N_B = 1$, and $N_U > 1$: Without a time and frequency offset, there is enough information to find the 3D position of the receiver using: i) two TOAs from the same LEO satellite obtained during two distinct time slots in combination with the Doppler measurements obtained during either of the time slots with respect to the LEO satellite, and ii) two Doppler measurements obtained during the two distinct time slots with respect to the LEO satellite in combination with the TOA obtained during either of the time slots. iii) two unit vectors obtained during the two distinct time slots from the same LEO satellite obtainable due to the presence of multiple receive antennas, iv) one TOA measurement from the LEO during either of the time slots and a unit vector from the LEO during either of the time slots and v) one Doppler measurement from the LEO during either of the time slots and a unit vector from the other LEO during either of the time slots.

7) $N_K = 3$, $N_B = 1$, and $N_U > 1$: Without a time and frequency offset, there is enough information to find the 3D position of the receiver using: i) three TOA measurements obtained during three different time slots from a single LEO satellite, ii) three Doppler measurements obtained during three different time slots from a single LEO satellite, iii) two TOAs from the same LEO satellite obtained during two distinct time slots in combination with the Doppler measurements obtained during either of the time slots with respect to the LEO satellite, and iv) two Doppler measurements obtained during the two distinct time slots with respect to the LEO satellite in combination with the TOA obtained during either of the time slots. v) two unit vectors obtained during the two distinct time slots from the same LEO satellite obtainable due to the presence of multiple receive antennas, vi) one TOA measurement from the LEO during either of the time slots and a unit vector from the LEO during either of the time slots, and vii) one Doppler measurement from the LEO during either of the time slots and a unit vector from the other LEO during either of the time slots. With only a time offset, ii) can be used to find the 3D position. With only a frequency offset, i), v), and vi) can be used to find the 3D position.

We next present cases for $N_K > 3$. These cases are unique and special because they allow time and frequency difference techniques to handle scenarios with both time and frequency offsets.

8) $N_K = 4$, $N_B = 1$, and $N_U = 1$: Without a time and frequency offset, there is enough information to find the 3D position of the receiver using: i) four TOA measurements obtained during four different time slots from a single LEO satellite with one of the TOA measurements serving as a reference measurement for time differencing, ii) four Doppler measurements obtained during four different time slots from a single LEO satellite with one of the Doppler measurements serving as a reference measurement for frequency differencing, iii) three TOA measurements obtained during three different time slots from a single LEO satellite, iv) three Doppler measurements obtained during three different time slots from a single LEO satellite, v) two TOAs from the same LEO satellite obtained during two distinct time slots in combination with the Doppler measurements obtained during either of the time slots with respect to the LEO satellite, and vi) two Doppler measurements obtained during the two distinct time slots with respect to the LEO satellite in combination with the TOA obtained during either of the time slots. While with a time offset, i), ii), and iv) can be used to provide the 3D position of the receiver, with a frequency offset, i), ii), and iii) can be used to provide the 3D position of the receiver. With both a time and frequency offset, i) and ii) can be used to provide the 3D position of the receiver.

9) $N_K = 4$, $N_B = 1$, and $N_U > 1$: Without a time and frequency offset, there is enough information to find the 3D position of the receiver using: i) four TOA measurements obtained during four different time slots from a single LEO satellite with one of the TOA measurements serving as a reference measurement for time differencing, ii) four Doppler measurements obtained during four different time slots from a single LEO satellite with one of the Doppler measurements serving as a reference measurement for frequency differencing, iii) three TOA measurements obtained during three different time slots from a single LEO satellite, iv) three Doppler measurements obtained during three different time slots from a single LEO satellite, v) two TOAs from the same LEO satellite obtained during two distinct time slots in combination with the Doppler measurements obtained during either of the time slots with respect to the LEO satellite, and vi) two Doppler measurements obtained during the two distinct time slots with respect to the LEO satellite in combination with the TOA obtained during either of the time slots. vii) two unit vectors obtained during the two distinct time slots from the same LEO satellite obtainable due to the presence of multiple receive antennas, viii) one TOA measurement from the LEO during either of the time slots and a unit vector from the LEO during either of the time slots and ix) one Doppler measurement from the LEO during either of the time slots and a unit vector from the LEO during either of the time slots. With only a time offset, i) ii), and iv) can be used to find the 3D position. With only a

frequency offset, i), ii), (iii), (vii), and viii) can be used to find the 3D position. When both a time offset and frequency offset are present, i) and ii) can be used to find the 3D position.

B. Simulation results

Here, we present simulation results for the CRLB when estimating $\boldsymbol{p}_U$ with $N_K = 4$, $N_B = 1$, *and* $N_U > 1$. In Fig. 2, we notice an improvement in positioning error due to an increase in the length of the time interval between the transmission time slots is more clearly seen. This reduction in positioning error is slow from 25 ms to 100 ms but is drastic above 100 ms. This improvement in positioning error is due to the speed of the LEO satellites. The speed of satellites means that the same satellite can act as multiple anchors in different time slots while still achieving good geometric dilution of precision.

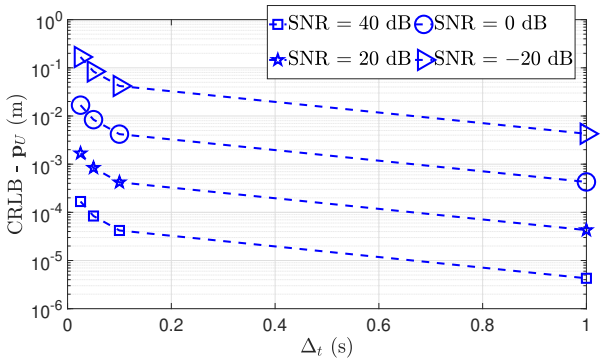

Figure 2. CRLB for $\boldsymbol{p}_U$ with $f_c = 40$ GHz and $N_U = 4$: focuses on Δ_t values from $\Delta_t = 25$ ms to $\Delta_t = 1$ s.

VI. Conclusion

In this paper, we have explored the fundamental limits of positioning performance using signals from unsynchronized LEO satellites. This analysis has shed light on the relationship between the number of signals needed, the operating frequency, the number of time slots received and the number of received antennas in order to obtain 3D position. One key result is that when the LEOs are unsynchronized with each other in time and frequency and experience a high Doppler rate, the 3D position can be determined by observing a single LEO for 4 transmission time slots, which are spaced at least 25 ms.

Appendix

A. Entries in transformation matrix

The derivative of the delay from the u^{th} receive antenna to the b^{th} LEO satellite during the k^{th} time slot with respect to the $\boldsymbol{p}_U$ is simply the unit vector from the u^{th} receive antenna to the b^{th} LEO satellite during the k^{th} time slot normalized by the speed of light. This is represented next. $\nabla_{\boldsymbol{p}_U}\tau_{bu,k} \triangleq \nabla_{\boldsymbol{p}_U}\frac{\|\mathbf{p}_{u,k}-\mathbf{p}_{b,k}\|}{c} = \nabla_{\boldsymbol{p}_U}\frac{\boldsymbol{d}_{bu,k}}{c} = \frac{\boldsymbol{\Delta}_{bu,k}}{c}$. The derivative of the Doppler observed at the receiver measured from the b^{th} LEO satellite during the k^{th} time slot with respect to $\boldsymbol{p}_U$ is $\nabla_{\boldsymbol{p}_U}\nu_{b,k} \triangleq \frac{(\boldsymbol{v}_B-\boldsymbol{v}_U)-\boldsymbol{\Delta}_{bU,k}^{\mathrm{T}}(\boldsymbol{v}_B-\boldsymbol{v}_U)\boldsymbol{\Delta}_{bU,k}}{\boldsymbol{d}_{bU,k}^{-1}}$.

References

[1] J. Kang, P. E. N, J. Lee, H. Wymeersch, and S. Kim, "Fundamental performance bounds for carrier phase positioning in LEO-PNT systems," in *Proc., IEEE Intl. Conf. on Acoustics, Speech, and Sig. Proc. (ICASSP)*, 2024, pp. 13 496–13 500.

[2] T. Reid, A. Neish, T. Walter, and P. Enge, "Broadband LEO constellations for navigation," *Navigation*, vol. 65, Jun. 2018.

[3] P. A. Iannucci and T. E. Humphreys, "Economical fused LEO GNSS," in *Proc., IEEE/ION Position, Location and Navigation Symposium (PLANS)*, 2020, pp. 426–443.

[4] A. Nardin, F. Dovis, and J. A. Fraire, "Empowering the tracking performance of LEO-based positioning by means of meta-signals," *IEEE J. of Radio Frequency Identification*, vol. 5, no. 3, pp. 244–253, Sep. 2021.

[5] D. Egea-Roca, J. López-Salcedo, G. Seco-Granados, and E. Falletti, "Performance analysis of a multi-slope chirp spread spectrum signal for pnt in a LEO constellation," in *proc., Satellite Navigation Technology Workshop (NAVITEC)*, 2022, pp. 1–9.

[6] L. You, X. Qiang, Y. Zhu, F. Jiang, C. G. Tsinos, W. Wang, H. Wymeersch, X. Gao, and B. Ottersten, "Integrated communications and localization for massive MIMO LEO satellite systems," *IEEE Trans. on Wireless Commun.*, to appear.

[7] M. L. Psiaki, "Navigation using carrier doppler shift from a LEO constellation: TRANSIT on steroids," *NAVIGATION*, vol. 68, no. 3, pp. 621–641, 2021. [Online]. Available: https://onlinelibrary.wiley.com/doi/abs/10.1002/navi.438

[8] J. Khalife, M. Neinavaie, and Z. M. Kassas, "Navigation with differential carrier phase measurements from megaconstellation LEO satellites," in *Proc., IEEE/ION Position, Location and Navigation Symposium (PLANS)*, 2020, pp. 1393–1404.

[9] J. Haidar-Ahmad, N. Khairallah, and Z. M. Kassas, "A hybrid analytical-machine learning approach for LEO satellite orbit prediction," in *proc., International Conference on Information Fusion (FUSION)*, 2022, pp. 1–7.

[10] M. Neinavaie, J. Khalife, and Z. M. Kassas, "Acquisition, doppler tracking, and positioning with starlink LEO satellites: First results," *IEEE Trans. on Aerospace and Electronic Systems*, vol. 58, no. 3, pp. 2606–2610, Apr. 2022.

[11] Z. M. Kassas, N. Khairallah, and S. Kozhaya, "Ad astra: Simultaneous tracking and navigation with megaconstellation LEO satellites," *IEEE Aerospace and Electronic Systems Magazine*, to appear.

[12] M. Neinavaie and Z. M. Kassas, "Cognitive sensing and navigation with unknown OFDM signals with application to terrestrial 5G and starlink LEO satellites," *IEEE J on Selected Areas in Commun.*, vol. 42, no. 1, pp. 146–160, Jan. 2024.

[13] R. Sabbagh and Z. M. Kassas, "Observability analysis of receiver localization via pseudorange measurements from a single LEO satellite," *IEEE Control Systems Lett.*, vol. 7, pp. 571–576, Jun. 2023.

[14] S. E. Kozhaya and Z. M. Kassas, "Positioning with starlink LEO satellites: A blind Doppler spectral approach," in *IEEE 97th Vehicular Technology Conference (VTC2023-Spring)*, 2023, pp. 1–5.

[15] J. J. Khalife and Z. M. Kassas, "Receiver design for Doppler positioning with LEO satellites," in *IEEE International Conference on Acoustics, Speech and Signal Processing (ICASSP)*, 2019, pp. 5506–5510.

[16] M. Neinavaie and Z. M. Kassas, "Unveiling starlink LEO satellite OFDM-like signal structure enabling precise positioning," *IEEE Trans. on Aerospace and Electronic Systems*, vol. 60, no. 2, pp. 2486–2489, Apr. 2024.

[17] S. M. LaValle, *Planning Algorithms*. Cambridge University Press, 2006.

[18] Y. Shen and M. Z. Win, "Fundamental limits of wideband localization — part I: A general framework," *IEEE Trans. on Info. Theory*, vol. 56, no. 10, pp. 4956–4980, Oct. 2010.

[19] S. M. Kay, *Fundamentals of Statistical Signal Processing: Estimation Theory*. Prentice-Hall, Inc., 1993.